

## Supplementary Information

### Rational Design of Double-Shelled Cu<sub>2</sub>MoS<sub>4</sub>@N-Doped Carbon Hierarchical Nanoboxes Toward Fast and Stable Sodium-Ion Batteries

Bo Yan,<sup>a</sup> Lichen Lin,<sup>b</sup> Chang Sun,<sup>a</sup> Lin Gao,<sup>a</sup> Huachao Tao,<sup>a</sup> Lulu Zhang,<sup>a</sup> Shengkui Zhong,<sup>c</sup>  
Xifei Li,\*<sup>d</sup> Xuelin Yang\*<sup>a</sup>

<sup>a</sup>*Collaborative Innovation Center for Microgrid of New Energy, College of Electrical Engineering & New Energy, China Three Gorges University, Yichang 443002, P. R. China.*

<sup>b</sup>*College of Materials and Chemical Engineering, China Three Gorges University, Yichang 443002, P. R. China.*

<sup>c</sup>*School of Marine Science and Technology, Hainan Tropical Ocean University, Hainan 572000, P. R. China.*

<sup>d</sup>*Xi'an Key Laboratory of New Energy Materials and Devices, Institute of Advanced Electrochemical Energy & School of Materials Science and Engineering, Xi'an University of Technology, Xi'an, Shaanxi, 710048, P. R. China.*

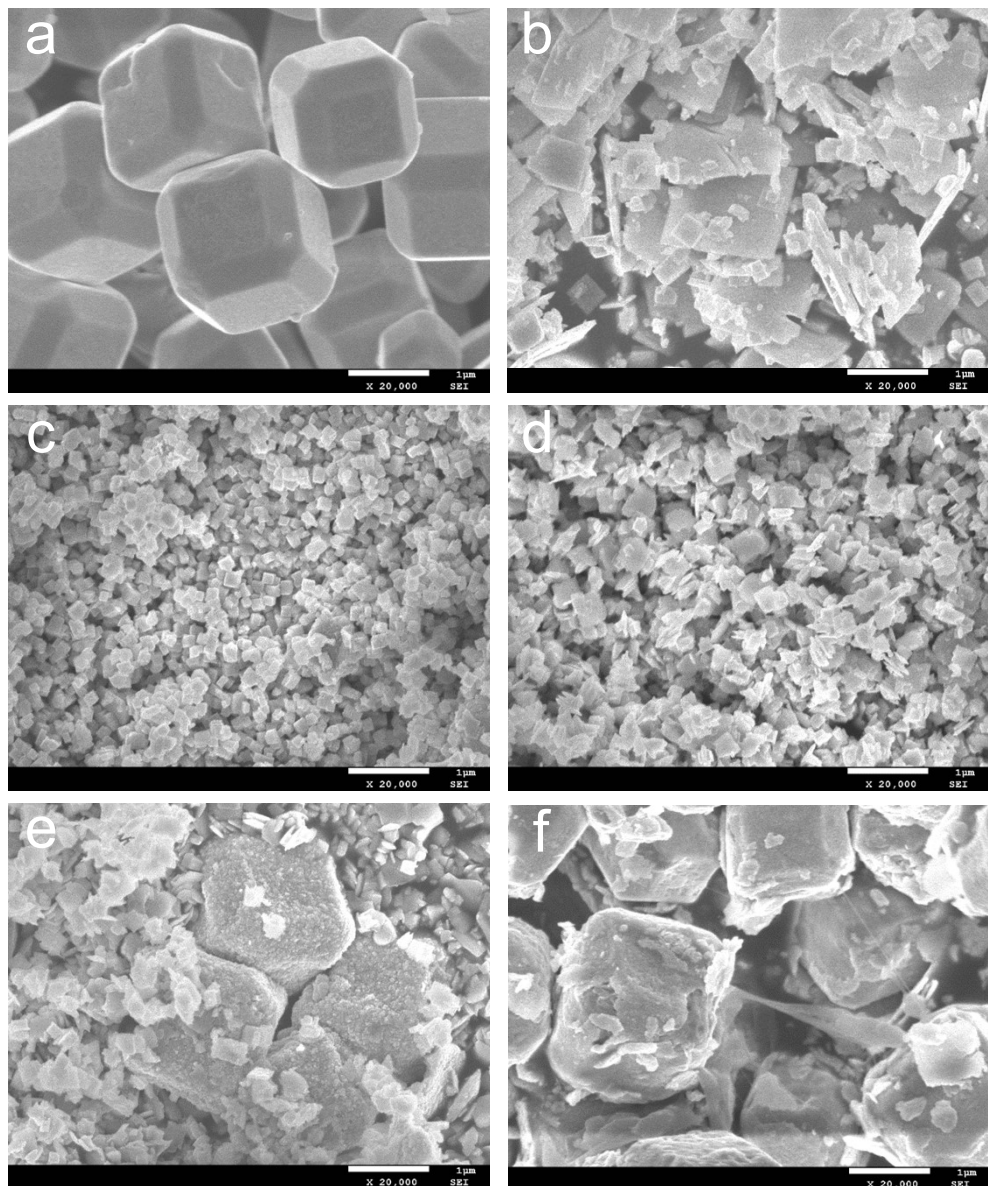


**Fig. S1** Morphology evolution of Cu<sub>2</sub>O nanocubes reaction with Na<sub>2</sub>MoO<sub>4</sub> and TAA under different high temperature pressure conditions: a) non-reaction, b) 200 °C-30 h, c) 180 °C-18 h, d) 160 °C-12 h, e) 160 °C-2 h, and f) 140°C-2 h.

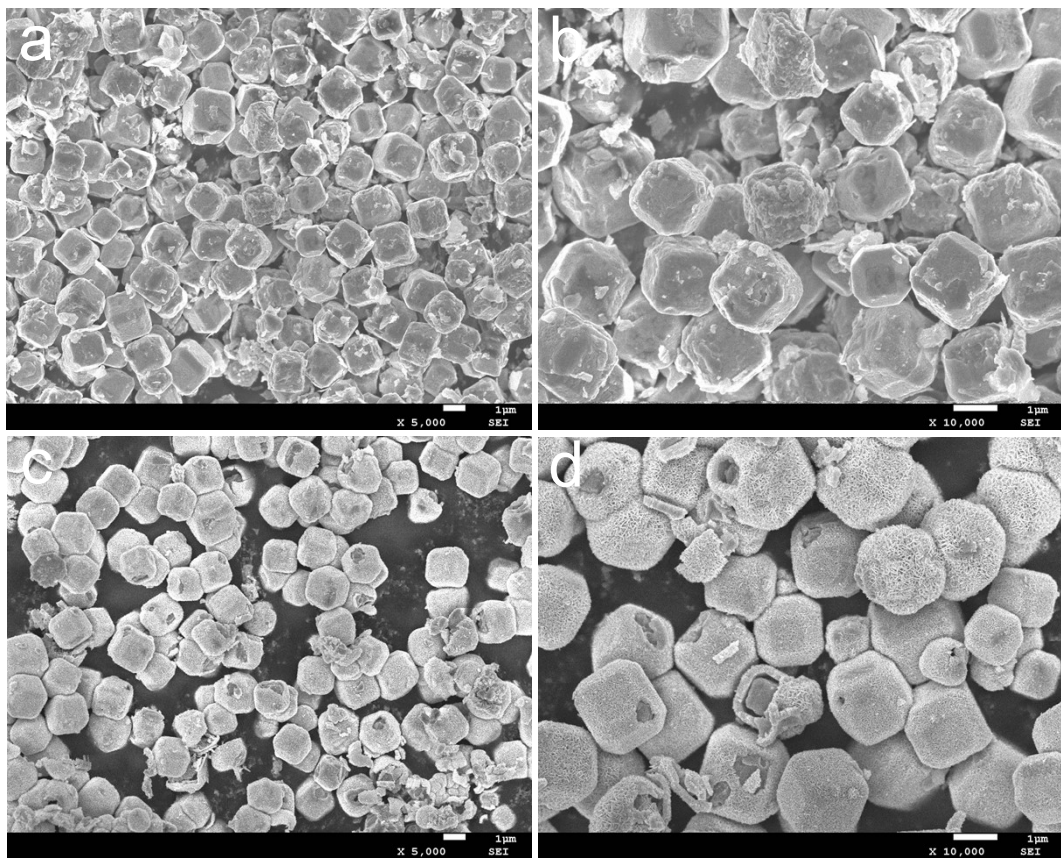


**Fig. S2** Low- and high-magnification FESEM images of  $\text{Cu}_2\text{O}$  nanocubes reaction with  $\text{Na}_2\text{MoO}_4$  and TAA under solvothermal condition of (a, b) 140 °C for 2 h and (c, d) 140 °C for 24 h.

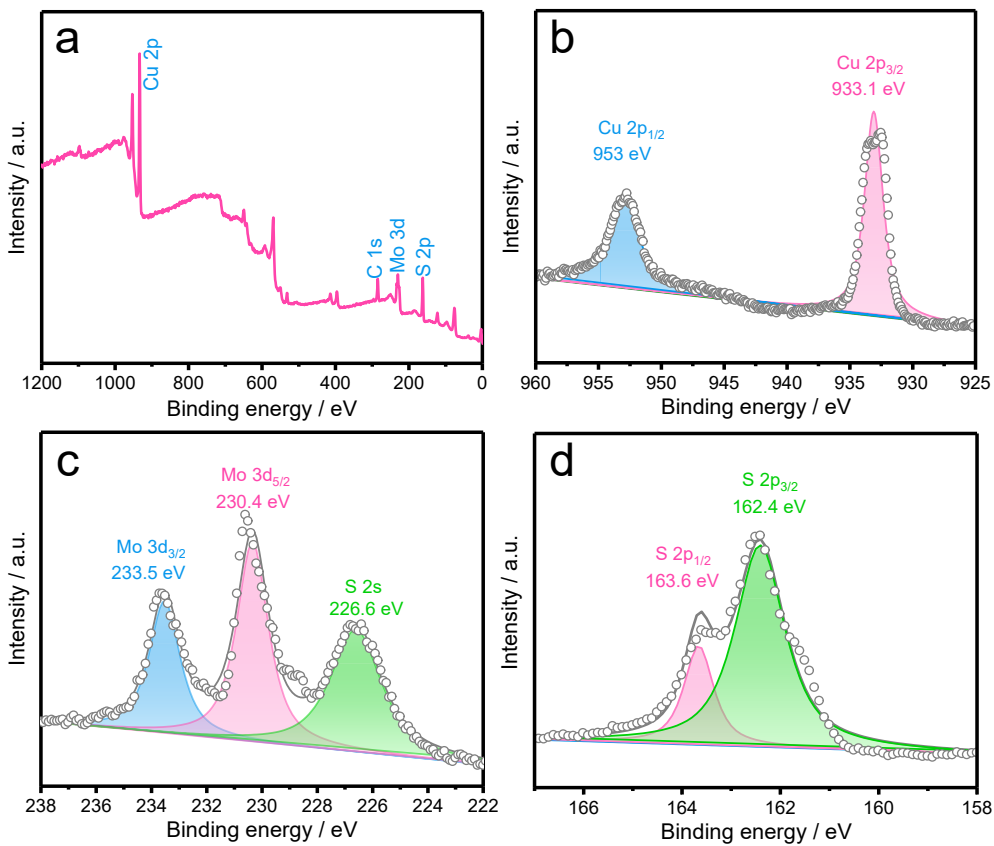


**Fig. S3** Characterization of the pristine  $\text{Cu}_2\text{MoS}_4$  nanoboxes: a) the integrated XPS spectrum, and the corresponding high-resolution XPS spectra of b) Cu 2p, c) Mo 3d, and d) S 2p.

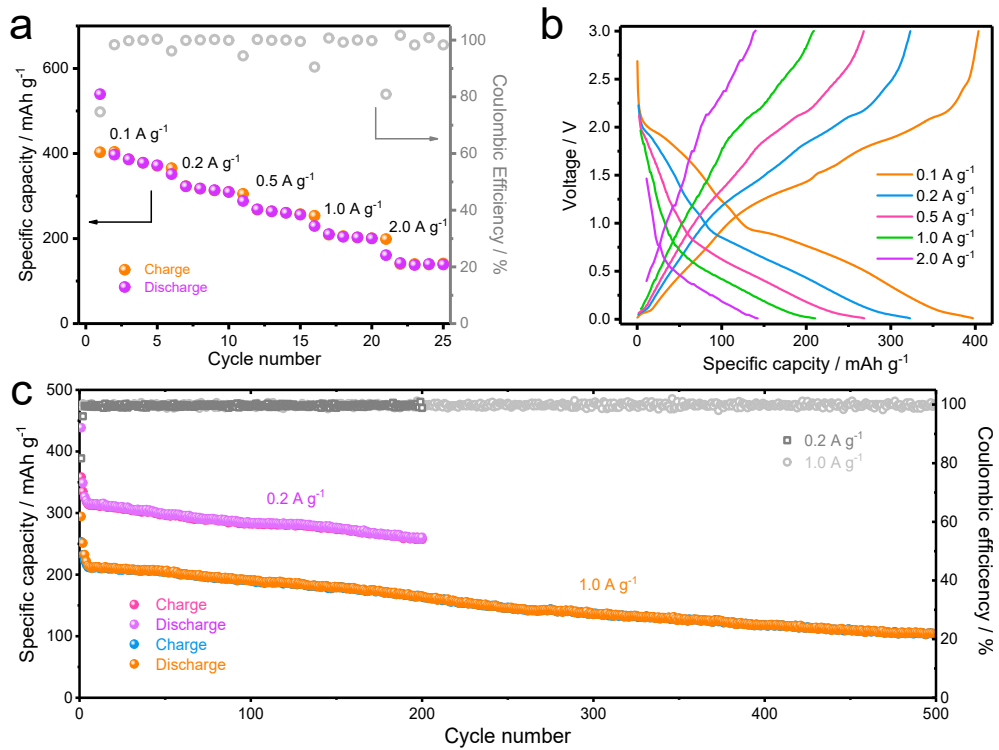


**Fig. S4** Electrochemical evaluation of Cu<sub>2</sub>MoS<sub>4</sub>. a) Rate capabilities ranging from 0.1 to 2.0 A g<sup>-1</sup>. b) Voltage profiles at various current densities from 0.1 to 2.0 A g<sup>-1</sup>. c) Prolonged cycle life and Coulombic efficiency at 0.2 and 1.0 A g<sup>-1</sup>.

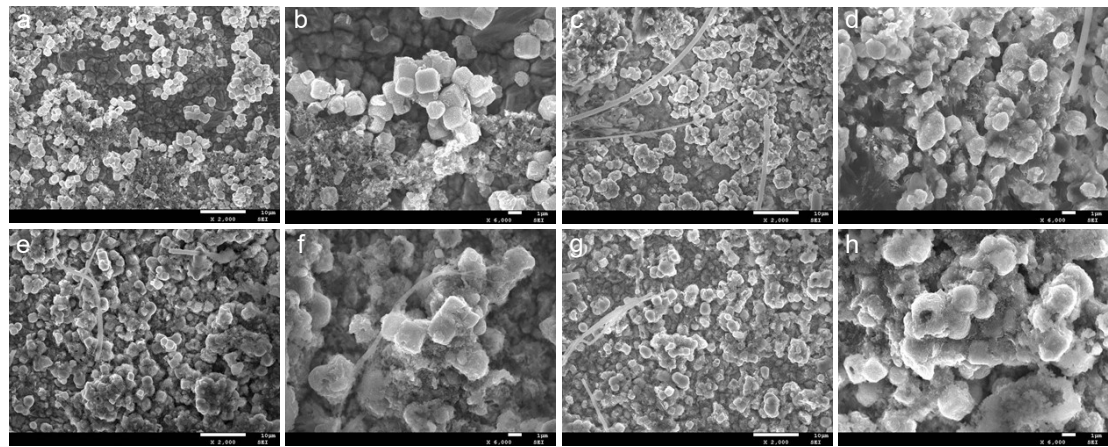


**Fig. S5** FESEM images of a, b) Cu<sub>2</sub>MoS<sub>4</sub> electrode and e, f) Cu<sub>2</sub>MoS<sub>4</sub>@NC electrode before cycling. FESEM images of c, d) Cu<sub>2</sub>MoS<sub>4</sub> electrode and g, h) Cu<sub>2</sub>MoS<sub>4</sub>@NC electrode after 500 cycles at a current density of 1.0 A g<sup>-1</sup>.

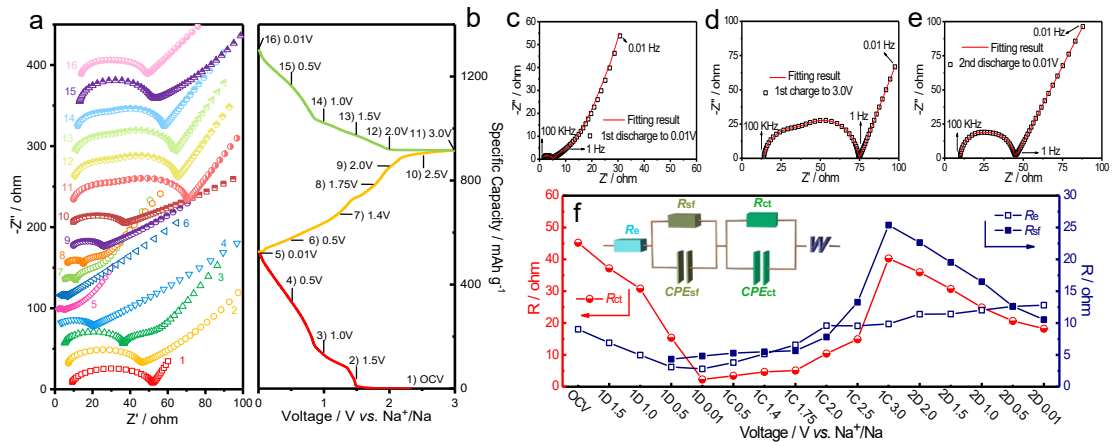


**Fig. S6** Electrochemical reaction kinetic of Cu<sub>2</sub>MoS<sub>4</sub>. a) Nyquist plots collected at each point marked on (b) in the frequency range of 100 kHz to 10 mHz. b) Discharge-charge curves: each point represents an EIS measurement. Typical Nyquist plots collected at c) 1st discharge to 0.01 V, d) 1st charge to 3.0 V, and e) 2nd discharge to 0.01 V. f) EIS parameters derived from the equivalent circuit (inset of f).

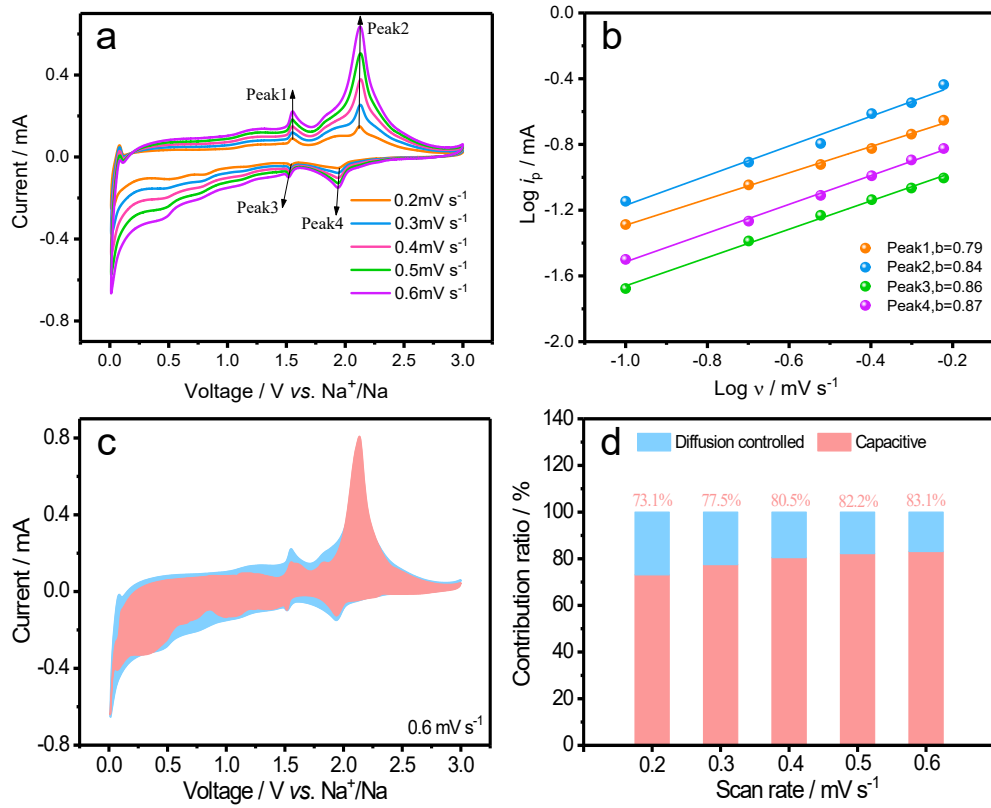


**Fig. S7** Electrochemical reaction kinetic of  $\text{Cu}_2\text{MoS}_4$ . a) CV curves at various scan rates. b) Determination of the b value using the relationship between peak current and scan rate. c) Separation of the capacitive and diffusion currents at a scan rate of 0.6  $\text{mV s}^{-1}$  with the capacitive fraction shown by the shaded region. d) Contribution ratio of the capacitive and diffusion-controlled charge versus scan rate.

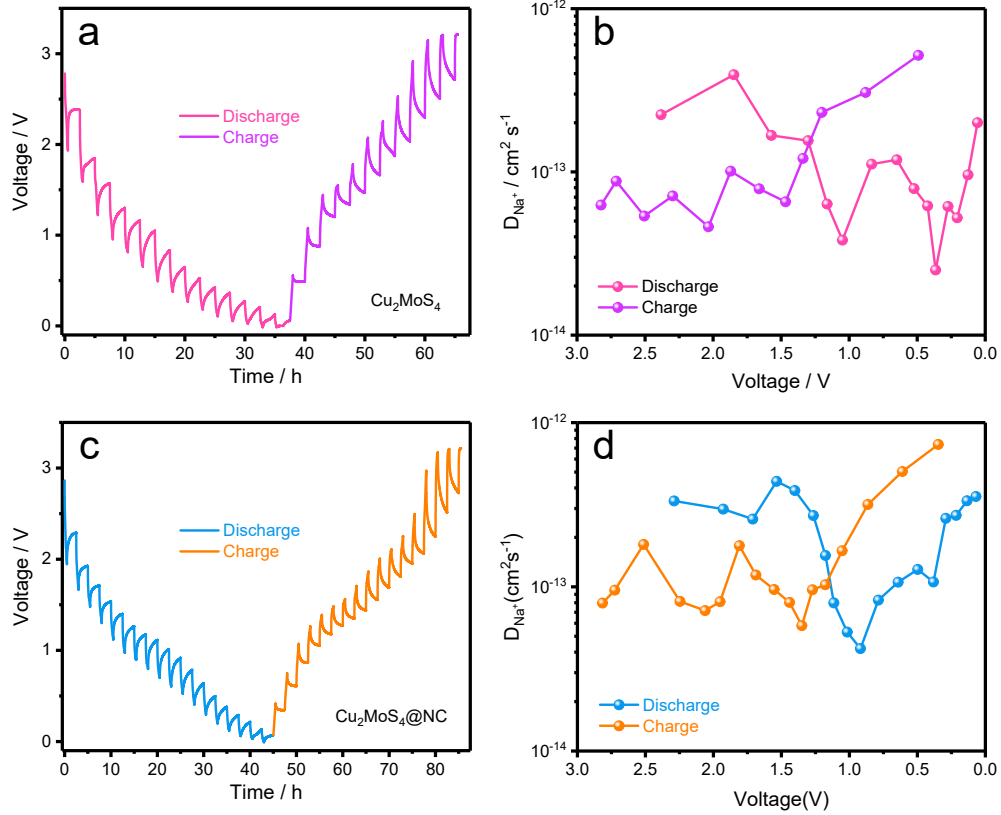


**Fig. S8** a) GITT curves and b) calculation of  $\text{Na}^+$  diffusion coefficients at different discharge/charge states of  $\text{Cu}_2\text{MoS}_4$  electrode. c) GITT curves and d) calculation of  $\text{Na}^+$  diffusion coefficients at different discharge/charge states of  $\text{Cu}_2\text{MoS}_4@\text{NC}$  electrode.

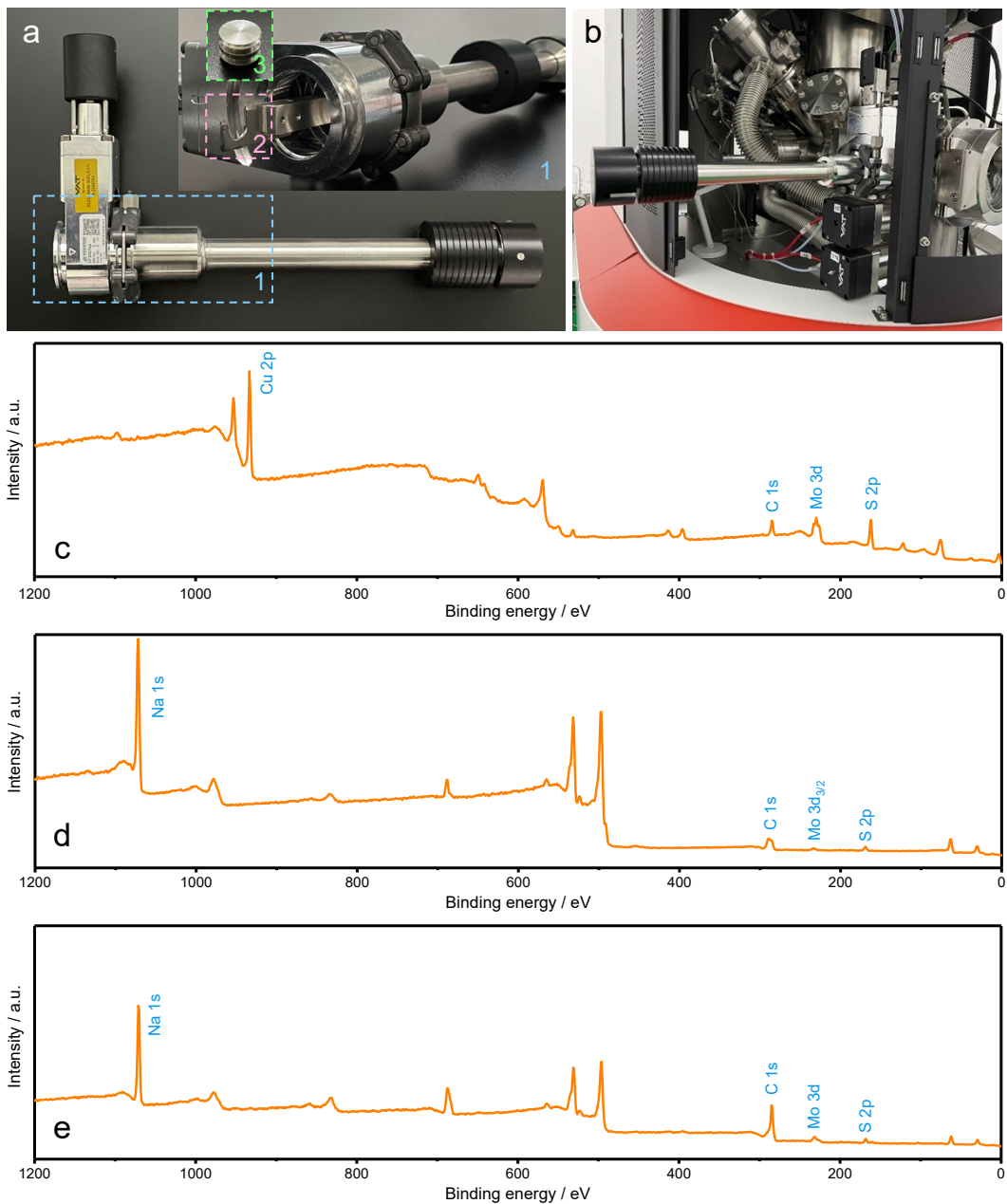


**Fig. S9** a) Structure and b) working position of sample transfer lever. Ex-situ XPS spectra of c)  $\text{Cu}_2\text{MoS}_4@\text{NC}$  before cycling, d)  $\text{Cu}_2\text{MoS}_4@\text{NC}$  electrode at the initial discharge state of 0.01 V, and e)  $\text{Cu}_2\text{MoS}_4@\text{NC}$  electrode at the initial charge state of 3.0 V.

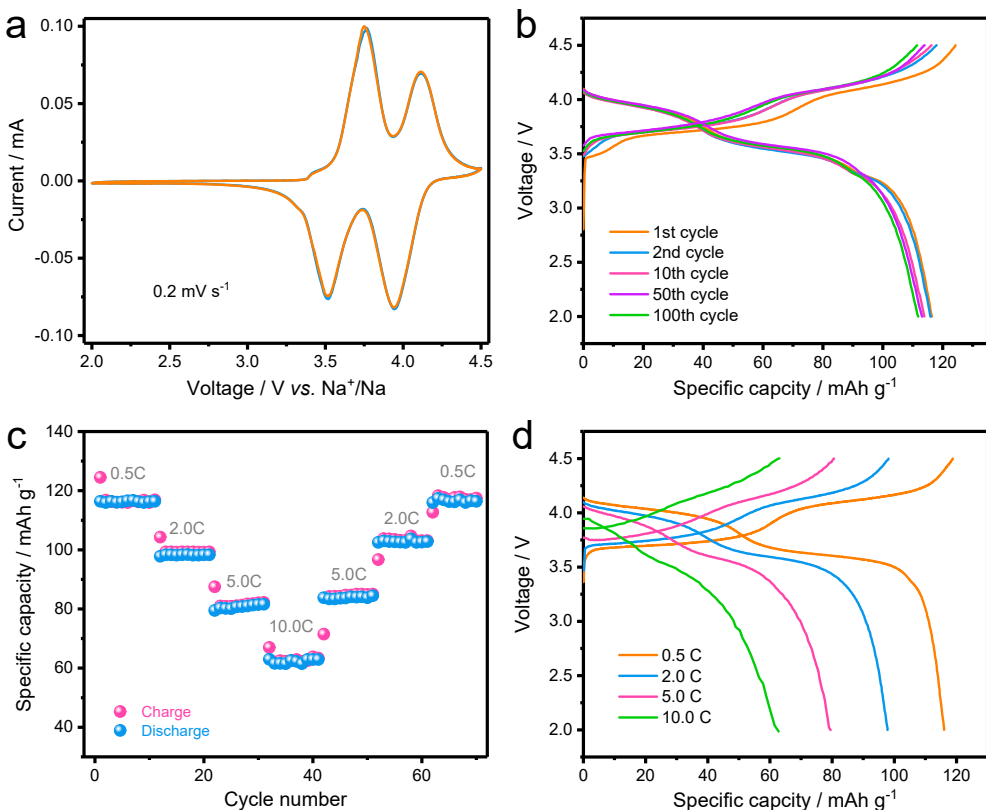


**Fig. S10** Electrochemical evaluation of  $\text{Na}_3\text{V}_2(\text{PO}_4)_2\text{F}_3/\text{C}$  cathode. a) CV curves at  $0.2 \text{ mV s}^{-1}$  with the voltage range of 2.0~4.5 V. b) Galvanostatic charge/discharge profiles at 0.5 C. c) Rate capabilities ranging from 0.5 to 10 C. b) Voltage profiles at various current rates from 0.5 to 10 C. The  $\text{Na}_3\text{V}_2(\text{PO}_4)_2\text{F}_3/\text{C}$  was synthesized according to our previously reported method (doi: 10.1021/acsami.8b10299) with an appropriate modification.

**Table S1** Electrochemical performances of Cu<sub>2</sub>MoS<sub>4</sub>@NC compared with other previously-reported metal-sulfides based anode materials for SIBs.

Metallic sulfides	Cut-off voltage	Current density	Capacity retention (%)	Rate capacity (mAh g <sup>-1</sup> ) / current density	Ref.
Bi <sub>2</sub> S <sub>3</sub> /MoS <sub>2</sub>	0.01-3.0	0.5 A/g	65 (after 100 cycles)	427.9 at 0.2 A/g	[S1]
Ni–Fe bimetallic sulfide nanoflakes@ carbon	0.001-3.0	0.2 A/g	51 (after 250 cycles)	443 at 0.2 A/g 278 at 2.0 A/g	[S2]
WS <sub>2-x</sub> /ZnS@C	0.01-3.0	1.0 A/g	62 (after 500 cycles)	468.2 at 0.1 A/g 251.4 at 2.0 A/g	[S3]
N/S-rGO@ ZnSnS <sub>3</sub>	0.01-3.0	1.0 A/g	68 (after 500 cycles)	256.6 at 2.0 A/g	[S4]
In <sub>2</sub> S <sub>3</sub> -Sb <sub>2</sub> S <sub>3</sub> @MCNTs	0.01-2.5	0.2 A/g 0.4 A/g	54 (after 100 cycles) 46 (after 500 cycles)	467 at 0.2 A/g	[S5]
Ti <sub>0.25</sub> Sn <sub>0.75</sub> S <sub>2</sub> @ MWCNTs	0.01-2.5	0.4 A/g	45 (after 200 cycles)	364 at 0.8 A/g	[S6]
Prussian blue analogs derived (CoFe)S <sub>x</sub> @C	0.01-3.0	0.5 A/g	14 (after 160 cycles)	480 at 0.1 A/g 200 at 2.0 A/g	[S7]
CoS <sub>2</sub> @Cu <sub>x</sub> S	0.4-2.6	0.3 A/g	70.6 (after 300 cycles)	410 at 0.1 A/g	[S8]
Cu <sub>2</sub> ZnSnS <sub>4</sub> @C	0.01-3.0	0.05 A/g 1.0 A/g	61 (after 140 cycles) 72 (after 250 cycles)	400 at 0.2 A/g 243 at 2.0 A/g	[S9]

$\text{Cu}_2\text{MoS}_4$ -rGO hollow nanospheres	0.5-3.0	0.5 A/g	83 (after 200 cycles)	260 at 0.1 A/g 193 at 2.0 A/g	[S10]
$\text{Cu}_2\text{S}@\text{Carbon}$ $@\text{MoS}_2$	0.2-3.0	0.3 A/g	53 (after 200 cycles)	316 at 2.0 A/g	[S11]
$\text{Cu}_2\text{MoS}_4@\text{NC}$	0.01-3.0	0.2 A/g 1.0 A/g	72 (after 200 cycles) 74 (after 500 cycles)	492 at 0.1 A/g 302 at 2.0 A/g	This Work

**Table S2** Fitting parameters of  $\text{Cu}_2\text{MoS}_4@\text{NC}$  anode charged to 2.0 V in the 1st cycle.

Electrolyte	$R_e$	1.498 $\Omega$
SEI	$R_{sf}$ $CPE_{sf}T$ $CPE_{sf}P$	2.814 $\Omega$ 1.049E-5 0.8561
Charge transfer	$R_{ct}$ $CPE_{ct}T$ $CPE_{ct}P$	2.417 $\Omega$ 3.582E-5 0.5794
Diffusion	$R_d$ of $W_{dif}$ $T$ of $W_{dif}$ $P$ of $W_{dif}$	806.4 $\Omega$ 3.043 1.035

## References

- S1 L. Cao, X. Liang, X. Ou, X. Yang, Y. Li, C. Yang, Z. Lin, M. Liu, *Adv. Funct. Mater.*, 2020, **30**, 1910732.
- S2 S. Yang, S. K. Park, G. D. Park, J. H. Kim, Y. Kang, *Chem. Eng. J.*, 2021, **417**, 127963.
- S3 Y. Li, J. Qian, M. Zhang, S. Wang, Z. Wang, M. Li, Y. Bai, Q. An, H. Xu, F. Wu, L. Mai, C. Wu, *Adv. Mater.*, 2020, **32**, 2005802.
- S4 X. Liu, Y. Hao, J. Shu, H. B. M. K. Sari, L. Lin, H. Kou, J. Li, W. Liu, B. Yan, D. Li, J. Zhang, X. Li, *Nano Energy*, 2019, **57**, 414–423.
- S5 Y. Huang, Z. Wang, Y. Jiang, S. Li, M. Wang, Y. Ye, F. Wu, M. Xie, L. Li, R. Chen, *Adv. Sci.*, 2018, **5**, 1800613.
- S6 Y. Huang, M. Xie, Z. Wang, Y. Jiang, G. Xiao, S. Li, L. Li, F. Wu, R. Chen, *Energy Storage Mater.*, 2018, **11**, 100–111.
- S7 J. Chen, S. Li, V. P. Kumar, P. S. Lee, *Adv. Energy Mater.*, 2017, **7**, 1700180.
- S8 Y. Fang, D. Luan, Y. Chen, S. Gao, X. Lou, *Angew. Chem. Int. Ed.*, 2020, **59**, 2644–2648.
- S9 B. Sun, Q. Zhang, C. Zhang, W. Xu, J. Wang, G. Yuan, W. Lv, X. Li, N. Yang, *Adv. Energy Mater.*, 2021, **11**, 2100082.
- S10 J. Chen, L. Mohrhusen, G. Ali, S. Li, K. Chung, K. Al-Shamery, P. S. Lee, *Adv. Funct. Mater.*, 2019, **29**, 1807753.
- S11 Y. Fang, D. Luan, Y. Chen, S. Gao, X. Lou, *Angew. Chem. Int. Ed.*, 2020, **18**, 7245–7250.